Journal of Engineering and Applied Sciences 12 (20): 5136-5146, 2017
ISSN: 1816-949X

Flow and Heat Transfer of Nanofluid over a Dynamic Stretching Sheet with Non-linear Velocity and Thermal Radiation

[1]A.G. Madaki, [1]R. Roslan, [1]R. Kandasamy and [2]I. Hashim
[1]Centre for Research in Computational Mathematics, Faculty of Science,
Technology and Human Development, Universiti Tun Hussein Onn Malaysia,
86400 Batu Pahat, Johor, Malaysia
[2]School of Mathematical Sciences, Universiti Kebangsaan Malaysia,
43600 Bangi, Selangor, Malaysia

Abstract: This study has focused on the development of the mathematical model of the nonlinear differential equations with both Brownian motion and thermal radiation being present. The similarity variables were used to transform the nonlinear governing boundary layer equations into ordinary differential equations. The solutions to this problem were derived by using the Optimal Homotopy Asymptotic Method (OHAM) in which the Runge-Kutta fourth order method with shooting technique was also used to validate the accuracy of our results. In relation to the pertinent parameters on the velocity, temperature and concentration profiles such as Brownian, thermophoresis, magnetic, shape, heat source and thermal radiation parameters have all been studied and details are given in both tables and graphs, respectively. The results obtained are fascinatingly agreed with the numerical solutions along with the previously published study.

Key words: Nanofluid, variable thickness, thermal radiation, non-linear equations, Optimal Homotopy Asymptotic Method (OHAM), Runge-Kutta method

INTRODUCTION

The boundary layer flow over a dynamic stretching sheet is an often engaged case in many engineering processes. The heat treatments are also used in the manufacture of many other materials such as glass-fibre, paper production and cooling of metallic sheets or electronic chips amongst others. It also involves the use of heating or chilling, normally it requires an intense temperature to achieve the desired result such as hardening or softening of a material. Where the heat treatment techniques consist of annealing, case hardening, precipitation strengthening, quenching and tempering.

The study of boundary layer flow over a moving surface happens to be an amazing research area by many scholars (Elbashbeshy and Aldawody, 2000; Elbashbeshy and Bazid, 2003, 2000, 2004a, b) investigated the effect of internal heat generation on unsteady flow and thermal boundary layer thickness (Fang, 2008) studied the impact of uniform-shear flow on the boundary layers over a stretching surface. Many researchers have shown their profound interest in the boundary layer flow problem along the stretching sheet (Ali, 1995; Nazar *et al*., 2004; Ishak *et al*., 2009; Chiam, 1995; Vajravelu, 2001; Prasad *et al*., 2009; Cortell, 2008). The term nanofluid which was first coined by Choi (1995) in his bid to propose the new group of enhancing heat transfer fluid by dispersing nano-sized particles in a base fluid. Now a days, the use of nanofluid in the research field has grabbed the attention of many scholars out there for its ability to enhance heat transfer and many industrial applications. Amongst the collection of articles gathered for this study are (Hamad, 2011; Oztop and Abu Nada, 2008; Rana and Bhargava, 2012; Alsaedi *et al*., 2012; Khan and Pop, 2010; Fang *et al*., 2012; Chen and Char, 1988; Magyari and Keller, 2000; Nadeem *et al*., 2010). Recently, Abdel-wahed *et al*. (2015) analytically analyzed the influence of Brownian motion during the flow and heat transfer process in the nanofluid. Furthermore, more useful studies concerning the study of flow and heat transfer of nanofluid over a stretching sheet surface are recently available as duly reported by Zhang *et al*. (2016), Pourmehran *et al*. (2016), Eid (2016), Khan *et al*. (2015) Hayat *et al*. (2017) and Sui *et al*. (2016).

Radiation is a method of heat transfer that does not rely upon any contact between the heat source and the heated object as is the case with conduction and convection. Heat can be transmitted through empty space by thermal radiation often called infrared radiation. Moreover, Kandasamy *et al*. (2013) studied the thermal stratification due to solar energy radiation effects of the

Corresponding Author: R. Roslan, Centre for Research in Computational Mathematics, Faculty of Science, Technology and Human Development, Universiti Tun Hussein Onn Malaysia, 86400 Batu Pahat, Johor, Malaysia

unsteady Hiemenz flow of Cu-nanofluid over a porous wedge. Many studies in relation the thermal radiation effects can be found by Mustafa *et al.* (2015), Ashraf and Rashid (2012), Kothandapani and Prakash (2015), El-Arabawy (2003).

MATERIALS AND METHODS

In this study, we employed both analytical and numerical techniques, i.e. (OHAM) and Runge-Kutta fourth order along with shooting technique to derive the solution of hydromagnetic and radiative flow and heat transfer feature of a nanofluid over a dynamic stretching sheet with nonlinear velocity along the surface with Brownian motion, thermal radiation and other related parameters in the course of the heat treatment process.

Problem description: We consider the steady, laminar, two-dimensional boundary layer flow of an incompressible viscous nanofluid over a dynamic stretching sheet with a transverse magnetic field, heat generation and radiative heat flux. The surface is presumed to be far from being flat with certain features depending on the value of the shape parameter n which is defined as y = δ (x+b)1-n/2. The x-axis runs along the middle of the surface in the direction of its motion and the y-axis is perpendicular to it as shown in Fig. 1. Furthermore, it is assumed that both the fluid phase and nanoparticles are in thermal stability condition and no slip occurs between them.

We, therefore as sume the coefficient δ to be little in order to get the surface significantly narrows and the pressure gradients along the surface would be avoided while the induced magnetic field produced by the motion of an electrically conducting fluid is negligible. It is presumed that at the surface which is dynamic, the temperature T and the concentration of the nano-sized particle C bear constant values T_w and C_w respectively. While the surrounding values secured as y leans towards infinity of T and C are represented by T_∞ and C_∞ appropriately. Let U_w is the velocity of the dynamic surface.

Based on the usual boundary layer assumptions, the equations controls the two-dimensional incompressible hydro-magnetic nanofluid flow and heat transfer over a stretching sheet in the presence of thermal radiation can be written as:

$$\frac{\partial u}{\partial x}+\frac{\partial v}{\partial y}=0 \tag{1}$$

$$u\frac{\partial u}{\partial x}+v\frac{\partial u}{\partial y}=v\frac{\partial^2 u}{\partial y^2}-\frac{\sigma B^2(x)}{\rho}u \tag{2}$$

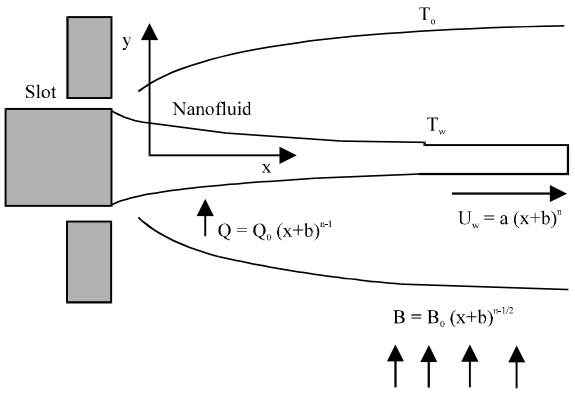

Fig. 1: Coordinate system and flow model

$$u\frac{\partial T}{\partial x}+v\frac{\partial T}{\partial y}=\alpha\frac{\partial^2 T}{\partial y^2}+\tau\left[D_B\frac{\partial C}{\partial y}\frac{\partial T}{\partial y}+\frac{D_T}{T_\infty}\left(\frac{\partial T}{\partial y}\right)^2\right]+\frac{Q(x)}{\rho C_P}(T-T_\infty)-\frac{1}{\rho C_P}\frac{\partial q_r}{\partial y} \tag{3}$$

$$u\frac{\partial C}{\partial x}+v\frac{\partial C}{\partial y}=D_B\frac{\partial^2 C}{\partial y^2}+\frac{D_T}{T_\infty}\left(\frac{\partial^2 T}{\partial y^2}\right) \tag{4}$$

Subject to boundary conditions:

$$u=U_w,\ v=0,\ T=T_w,\ C=C_w,\ \text{at}\ y=\delta(x+b)^{\frac{1-n}{2}},\qquad u=0,\ v=0,\ T=T_\infty,\ C=C_\infty\ \text{as}\ y\to\infty \tag{5}$$

Where:

u and v = Velocity components in x and y directions, respectively
ρ = The density of the base fluid
C_p = The heat capacity of a fluid at constant pressure
u = The kinematic viscosity
α = The thermal diffusion
σ = The electrical conductivity with D_B and D_T being the Brownian diffusion and thermophoretic diffusion coefficients
τ = The ratio between the effective heat capacity of the nanoparticle and heat capacity of the fluid
q_r = The radiative heat flux

While the certain form of the magnetic field B(x) = B_0 (x+b) n-1/2 and heat generation Q(x) = Q_0(x+b)n-1 are selected in order to get a similarity solution. While the expression of B (x) has been deliberated by Prasad *et al.* (2010). Introducing:

$$U_w(x) = \alpha(x+b)^n, \theta(\eta) = \frac{(T-T_\infty)}{(T_w-T_\infty)}, \varphi(\eta) = \frac{(C-C_\infty)}{(C_w-C_\infty)} \quad (6)$$

where, a and b are constants and n is the shape parameter. In this study, n+1>0 is presumed to authenticate the similarity variable and functions. The radiative heat flux in Eq. 3 is discussed by Rosseland (1931) as:

$$q_r = -\frac{4\sigma^*}{3k^*}\frac{\partial T^4}{\partial y} \quad (7)$$

where, α^* and k^* are the Stefan-Boltzmann constant and the mean absorption number, going by the study by Akbar *et al*. (2013), we presume that the temperature variation amidst the flow is significantly limited and the expression T^4 may be considered as a linear function of temperature. Therefore, T^4 is expanded using Taylor series expansion about T_∞ and ignoring the higher-order terms hence:

$$T^4 = 4T_\infty^3 T - 3T_\infty^4 \quad (8)$$

Using Eq. 7 and 8 into Eq. 3 we have:

$$u\frac{\partial T}{\partial x}+v\frac{\partial T}{\partial y} = \alpha\frac{\partial^2 T}{\partial y^2}+\tau\left[D_B\frac{\partial C}{\partial y}\frac{\partial T}{\partial y}+\frac{D_T}{T_\infty}\left(\frac{\partial T}{\partial y}\right)^2\right]+\frac{Q(x)}{\rho C_P}(T-T_\infty)+\frac{16\sigma^* T_\infty^3}{3\rho c_p k^*}\frac{\partial^2 T}{\partial y^2} \quad (9)$$

We consider the similarity solution of Eq. 2-4 subject to Eq. 5 in the following form:

$$\eta = y\sqrt{\left(\frac{n+1}{2}\right)\left(\frac{\alpha(x+b)^{n-1}}{\upsilon}\right)}, \psi = f(\eta)\sqrt{\left(\frac{2}{n+1}\right)(x+b)^{n+1}a\upsilon} \quad (10)$$

Where:

η = The similarity variable
ψ = The stream function which is defined as $u\,\partial_\psi/\partial_y$
∂_x/∂_ψ = That obviously satisfies Eq. 1

Putting Eq. 10 into Eq. 2-4 then the similarity equations are obtained as follows:

$$f'''+ff''-\left(\frac{2n}{n+1}\right)f'^2-\left(\frac{2}{n+1}\right)Mf' = 0 \quad (11)$$

$$(3+4PrN)\theta''+3Pr\left[f\theta'+\left(\frac{2}{n+1}\right)\lambda\theta+Nb\theta'\varphi'+Nt\theta'^2\right] = 0 \quad (12)$$

$$\varphi''+\frac{1}{2}Lef\varphi'+\left(\frac{Nt}{Nb}\right)\theta'' = 0 \quad (13)$$

with boundary conditions:

$$f(\alpha) = \alpha\left(\frac{1-n}{n+1}\right), f'(\alpha) = 1, \theta(0) = 1, \varphi(0) = 1 \text{ and } f'(\infty) = 0, \theta(\infty) = 0, \varphi(\infty) = 0 \quad (14)$$

where primes denote differentiation with respect to (η) where $\alpha = \delta n+\alpha/2u$ is the surface thickness parameter and at $\eta = \alpha$ pinpoints the plate surface. We defined $F(\xi) = f(\eta-\alpha) = f(\eta)$. Now the similarity Eq. 11-13 with their boundary Eq. 14 can be written as:

$$F'''+FF''-\left(\frac{2n}{n+1}\right)F'^2-\left(\frac{2}{n+1}\right)MF' = 0 \quad (15)$$

$$(3+4PrN)\theta''+3Pr\left[F\theta'+\left(\frac{2}{n+1}\right)\lambda\theta+Nb\theta'\varphi'+Nt\theta'^2\right] = 0 \quad (16)$$

$$\varphi''+\frac{1}{2}LeF\varphi'+\left(\frac{Nt}{Nb}\right)\theta'' = 0 \quad (17)$$

with boundary conditions:

$$F(0) = \alpha\left(\frac{1-n}{n+1}\right), F'(0) = 1, \theta(0) = 1, \varphi(0) = 1 \text{ and } F'(\infty) = 0, \theta(\infty) = 0, \varphi(\infty) = 0 \quad (18)$$

where the prime (') denotes differentiation with respect to (ξ) while the pertinent parameters are defined by:

$$Pr = \frac{\upsilon}{\alpha}, Le = \frac{\upsilon}{D_B}, M = \frac{B_0^2\sigma}{a\rho}, \lambda = \frac{Q_0}{a\rho c_p}, Nb = \frac{\tau D_B}{\upsilon}(C_w-C_\infty),$$
$$Nt = \frac{\tau D_T}{\upsilon T_\infty}(T_w-T_\infty), \tau = \frac{(\rho C_p)_P}{(\rho C_p)_f} \text{ and } N = \frac{4\sigma^* T_\infty^3}{\upsilon\rho C_P k^*}$$

Here Pr, Le, M, λ, Nb, Nt, τ and N represent the Prandtl number, the Lewis number, the magnetic field parameter, the heat source parameter, the Brownian motion parameter, the thermophoresis parameter, the ratio between the effective heat capacity of the nanoparticle material and heat capacity of the fluid and the thermal radiation parameter, respectively. In this study, the quantities of practical interest are the Nusselt number Nu, the skin friction coefficient C_{fx} and the Sherwood number Sh which are defined as:

$$Nu = \frac{(x+b)q_w}{k(T_w-T_\infty)} \Rightarrow Nu = -\sqrt{R_e}\sqrt{\frac{n+1}{2}}\theta'(0),$$
$$C_f = \frac{2\tau_w}{\rho U_w^2} \Rightarrow \sqrt{R_e}C_{fx} = 2\sqrt{\left(\frac{n+1}{2}\right)}F''(0),$$

$$Sh = \frac{(x+b)q_m}{D_B(C_w - C_\infty)} \Rightarrow Sh = -\sqrt{R_e}\frac{n+1}{2}\varphi'(0) \quad (19)$$

where, τ_w, q_w and q_m are the surface shear stress, surface heat flux and surface mass flux, respectively.

Analytical derivation using (OHAM): Here OHAM is being used to approximate the solution of the transformed ordinary differential Eq. 15-17 alongside Eq. 18 with respect to the suppositions:

$$F = F_0 + pF_1 + p^2F_2,\ H_1(p) = pC_1 + p^2C_2$$
$$\theta = \theta_0 + p\theta_1 + p^2\theta_2,\ H_2(p) = pC_3 + p^2C_4$$
$$\varphi = \varphi_0 + p\varphi_1 + p^2\varphi_2,\ H_3(p) = pC_5 + p^2C_6$$

where, $p \in [0, 1]$ is called an embedding parameter, $H_i(p)$, i = 1, 2 is a nonzero auxiliary function and C_i i = 1, 2, ..., 6 are constants (Marinca and Herisanu, 2008; Madaki *et al*., 2016).

Approximation of the momentum boundary layer equation: To apply OHAM on Eq. 15 with respect to 18, we consider the subsequent assumption as:

$$L = F''+F' \text{ and } N = F'''+FF'' - \left(\frac{2n}{n+1}\right)F'^2 - \left(\frac{2}{n+1}\right)MF' - F'' - F'$$

Where:
L = The linear operator
N = The non-linear operator

Applying OHAM to the Eq. 15 with respect to Eq. 18 we have:

$$(1-p)[F''+F'] = H_1(p)\left[F'''+FF'' - \left(\frac{2n}{n+1}\right)F'^2 - \left(\frac{2}{n+1}\right)MF'\right] \quad (20)$$

Using the boundary Eq. 18, after some simplification and equating the like powers of p-terms, we get; the zeroth-order equation p^0:

$$F_0'' + F_0' = 0, F_0(0) = a\left(\frac{1-n}{n+1}\right), F_0'(0) = 1 \quad (21)$$

The first-order equation p^1:

$$F_1'' + F_1' = F_0'' + F_0' + C_1\left[F_0''' + F_0F_0'' - \left(\frac{2n}{n+1}\right)F_0'^2 - \left(\left(\frac{2}{n+1}\right)M\right)\right]$$
$$F_0'\ F_1(0) = 0, F_1'(0) = 0 \quad (22)$$

The second-order equation p^2:

$$F_2'' + F_2' = F_1'' + F_1' + C_1\left[F_1''' + F_0F_1'' + F_1F_0'' - \left(\frac{4n}{n+1}\right)F_0'F_1' - \left(\left(\frac{2}{n+1}\right)M\right)F_1'\right] +$$
$$C_2\left[F_0''' + F_0F_0'' - \left(\frac{2n}{n+1}\right)F_0'^2 - \left(\left(\frac{2}{n+1}\right)M\right)F_0'\right],$$
$$F_2(0) = 0, F_2'(0) = 0 \quad (23)$$

Solving Eq. 21-23 with their corresponding boundary conditions, we obtained the approximation of $F_0(\xi)$, $F_1(\xi)$ and $F_2(\xi)$ as follows:

$$F_0(\xi) = -\frac{e^{-\xi}(1 - e^{\xi} + n - ne^{\xi} - \alpha e^{\xi} + \alpha ne^{\xi})}{1+n} \quad (24)$$

$$F_1(\xi) = \frac{C_1e^{-2\xi}\left(1 - n - e^{2\xi}(4M+n+2\alpha - 2n\alpha - 1) + 2e^{\xi}(2M(\xi+1) - (n-1)(\alpha\xi+\alpha-1))\right)}{2(1+n)} \quad (25)$$

$$F_2(\xi) = \begin{cases} \frac{1}{6(1+n)^2}(e^{-3\xi}(-6e^{\xi}(e^{\xi}-1)^2(n^2-1)C_1 + \\ (6e^{\xi}(n-1) - 3n^2 + 8n - 5(2 - 4M - 3\alpha + n(2+3\alpha)) - \\ 2e^{3\xi}(12M^2 - 12M(n-1)(\alpha-1) + (n-1)(3\alpha^2+9\alpha + \\ 3n - 11(\alpha^2 - 3\alpha - 1))) + 3e^{2\xi}(8M^2(\xi+1) - 8M(n-1) \\ (\alpha\xi+\alpha-2) + (n-1)(-2\alpha^2(\xi+1) + 12\alpha - 13 + \\ n(2\alpha^2(\xi+1) - 12\alpha - 5))))C_1^2 + 3e^{\xi}(n+1) \\ (1 - n - e^{2\xi}(-2n\alpha + 2\alpha + n + 4M - 1) + \\ 2e^{\xi}(2M(\xi+1) - (n-1)(\alpha\xi + \alpha - 1)))C_2)) \end{cases} \quad (26)$$

In general, the solution of Eq. 15 can be determined approximately in the form:

$$F(\xi) = F_0(\xi) + F_1(\xi) + F_2(\xi) \quad (27)$$

The residual equation in this case becomes:

$$R_1(\xi, C_1, C_2) = \left[F'''(\xi) + F(\xi)F''(\xi) - \left(\frac{2n}{n+1}\right)F'^2(\xi) - \left(\left(\frac{2}{n+1}\right)M\right)F'(\xi)\right] \quad (28)$$

The unknown constants C_1 and C_2 can be optimally identified from the conditions:

$$\frac{\partial J_1}{\partial C_1} = \frac{\partial J_1}{\partial C_2} = 0 \text{ where } J_1(C_i) = \int_0^{\infty} R_1^2(\xi, C_i)d\xi \quad (29)$$

Approximation of the energy boundary layer equation apply OHAM to the nonlinear Eq. 16 along the boundary Eq. 18, we consider the subsequent supposition:

$$L = \theta' + \theta \text{ and } N = \theta'' + \frac{3pr}{(3+4prN)}$$

$$[F\theta' + \left(\frac{2}{n+1}\right)\lambda\theta + Nb\theta'\varphi' + Nt\theta'^{2}] - [\theta' + \theta]$$

Where:
L = The linear operator
N = The non-linear operator

Applying OHAM to the Eq. 16 with respect to Eq. 18, we have:

$$(1-p)[\theta' + \theta] = H_1(p)\left[\theta'' + \frac{3Pr}{(3+4Pr\,N)}\left[F\theta' + \left(\frac{2}{n+1}\right)\lambda\theta + Nb\theta'\varphi' + Nt\theta'^{2}\right]\right] \quad (30)$$

Using the boundary Eq. 18 after some simplification and equating the like powers of P-terms, we get: the zeroth-order equation p^0:

$$\theta_0' + \theta_0 = 0,\ \theta_0(0) = 1 \quad (31)$$

The first-order equation p^1:

$$\theta_1' + \theta_1 = \theta_0' + \theta_0 + C_3\left[\theta_0'' + \frac{3Pr}{(3+4Pr\,N)}\left[F_0\theta_0' + \left(\frac{2}{n+1}\right)\lambda\theta_0 + Nb\theta_0'\varphi_0' + Nt\theta_0'^{2}\right]\right],\ \theta_1(0) = 0 \quad (32)$$

The second-order equation p^2:

$$\theta_2' + \theta_2 = \theta_1' + \theta_1 + C_3\left\{\theta_1'' + \frac{3Pr}{(3+4Pr\,N)}\left[F_0\theta_1' + F_1\theta_0' + \left(\frac{2}{n+1}\right)\lambda\theta_1 + Nb\theta_0'\varphi_1' + Nb\theta_1'\varphi_0' + 2Nt\theta_0'\theta_1'\right]\right\} + C_4\left\{\theta_0'' + \frac{3Pr}{(3+4Pr\,N)}\left[F_0\theta_0' + \left(\frac{2}{n+1}\right)\lambda\theta_0 + Nb\theta_0'\varphi_0' + Nt\theta_0'^{2}\right]\right\},\ \theta_2(0) = 0 \quad (33)$$

Solving Eq. 31-33 with their corresponding boundary conditions, we obtained the approximation of $\theta_0(\xi)$ and $\theta_1(\xi)$ as follows:

$$\theta_0(\xi) = e^{-\xi} \quad (34)$$

$$\theta_1(\xi) = \frac{1}{(1+n)(3+4PrN)}C_3e^{-2\xi}(3e^{\xi}(n+1)\xi + Pr(-3(n+1)(Nb+Nt+1) + e^{\xi}(3+3Nb+ 3Nt-3\xi+4N\xi-3\alpha\xi+n(3+3Nb+3Nt- 3\xi+4N\xi+3\alpha\xi)+6\xi\lambda))) \quad (35)$$

Similarly, $\theta_2(\xi)$ can be obtained from Eq. 33 now, the solution of Eq. 16 can be determined approximately in the form:

$$\theta(\xi) = \theta_0(\xi) + \theta_1(\xi) + \theta_2(\xi) \quad (36)$$

The residual equation in this case becomes:

$$R_2(\xi, C_3, C_4) = \theta''(\xi) + \frac{3Pr}{(3+4Pr\,N)}\left[F(\xi)\theta'(\xi) + \left(\frac{2}{n+1}\right)\lambda\theta(\xi) + Nb\theta'(\xi)\varphi'(\xi) + Nt\theta'^{2}(\xi)\right] \quad (37)$$

The unknown constants C_3 and C_4 can be optimally identified from the conditions:

$$\frac{\partial J_2}{\partial C_3} = \frac{\partial J_2}{\partial C_4} = 0$$

Where:

$$J_2(C_1) = \int_3^{\infty} R_2^2(\xi, C_1)d\xi \quad (38)$$

Approximation of the concentration boundary layer equation: Under the basis of the following assumptions, we can apply the OHAM to the nonlinear ordinary differential with the boundary (Eq. 18):

$$L = \varphi' + \varphi \text{ and } N = \varphi'' + \frac{1}{2}LeF\varphi' + \left(\frac{Nt}{Nb}\right)\theta'' - [\varphi' + \varphi]$$

Where:
L = The linear operator
N = The non-linear operator

Applying OHAM on with respect to Eq. 18, we have:

$$(1-p)[\varphi' + \varphi] = H_1(p)\left[\varphi'' + \frac{1}{2}LeF\varphi' + \left(\frac{Nt}{Nb}\right)\theta''\right] \quad (39)$$

Using the boundary Eq. 18 after some simplification and equating the like powers of p-terms, we get: the zeroth-order equation p^0:

$$\varphi_0' + \varphi_0 = 0,\ \varphi_0(0) = 1 \quad (40)$$

The first-order equation p^1:

$$\varphi_1' + \varphi_1 = \varphi_0' + \varphi_0 + C_5\left[\varphi_0'' + \frac{1}{2}LeF_0\varphi_0' + \left(\frac{Nt}{Nb}\right)\theta_0'\right],\ \varphi_1(0) = 0 \quad (41)$$

The second-order equation p^2:

$$\varphi_2' + \varphi_2 = \varphi_1' + \varphi_1 + C_5\left[\varphi_1'' + \frac{1}{2}LeF_0\varphi_1' + \frac{1}{2}LeF_1\varphi_0' + \left(\frac{Nt}{Nb}\right)\theta_1'\right] + C_6\left[\varphi_0'' + \frac{1}{2}LeF_0\varphi_0' + \left(\frac{Nt}{Nb}\right)\theta_0'\right],\ \varphi_2(0) = 0 \quad (42)$$

The solution of the zeroth-order and first-order Eq. 40 and 41 with their corresponding boundary conditions can be written as:

$$\varphi_0(\xi) = e^{-\xi} \quad (43)$$

$$\varphi_1(\xi) = \frac{1}{2(1+n)Nb}C_5e^{-2\xi}(-LeNb + e^{\xi}LeNb - nLeNb + e^{\xi}nLeNb + 2e^{\xi}Nb\xi - e^{\xi}LeNb\xi + 2e^{\xi}nNb\xi - e^{\xi}nLeNb\xi + 2e^{\xi}Nt\xi + 2e^{\xi}nNt\xi - e^{\xi}LeNb\alpha\xi + e^{\xi}nLeNb\alpha\xi) \quad (44)$$

Similarly, $\varphi_2(\xi)$ can be determined from Eq. 42. Now in general, the solution of Eq. 49 is therefore to be approximated using the expression:

$$\varphi(\xi) = \varphi_0(\xi) + \varphi_1(\xi) + \varphi_2(\xi) \quad (45)$$

The residual equation in this case becomes:

$$R_3(\xi, C_5, C_6) = \left[\varphi''(\xi) + \frac{1}{2}LeF(\xi)\varphi'(\xi) + \left(\frac{Nt}{Nb}\right)\theta''(\xi)\right] \quad (46)$$

The unknown constants C_5 and C_6 can be optimally identified from the conditions:

$$\frac{\partial J_3}{\partial C_5} = \frac{\partial J_3}{\partial C_6} = 0,\ \text{where } J_3(C_i) = \int_0^{\infty} R_3^2(\xi, C_i)d\xi \quad (47)$$

The results obtained for F" (0) in this study has been validated with the solutions obtained by Fang *et al.* (2012) (Table 1-5).

Table 1: Comparison of present results for -F" (0) at different values of n and α

		-F"(0)	
α	n	Previous study (Fang *et al.*, 2012)	Present study
0.25	0.0	0.7843	0.783031
	1.0	1.0000	1.000000
	3.0	1.0905	1.091060
	7.0	1.1323	1.132530
0.5	0.0	0.9576	0.956602
	1.0	1.0000	1.000000
	3.0	1.0359	1.036020
	7.0	1.0550	1.055080

Table 2: The effects of Nt on -θ' (0) and -φ' (0) along their associated Nu and Sh number when α = n = M = 0.60, Le = 2.0, Pr = 6.20, Nb = 0.10 and λ = 0.20 and N = 1.0

Nt	-θ' (0)	φ' (0)	Nu	Sh
0.1	0.034988	0.733114	-22.128	-463.662
0.4	0.110618	1.331927	-69.961	-842.385
0.6	0.176164	2.065176	-111.416	-1306.132

Table 3: The effects of λ on -θ' (0) and -φ' (0) along their associated, Nu and Sh number when α = n = M = N = 0.30, Le = 2.0, Pr = 6.20, Nt = Nb = 0.10

λ	-θ' (0)	φ' (0)	Nu	Sh
0.3	1.309267	0.400148	-746.397	-228.119
0.1	1.063156	0.173734	-606.092	-99.044
0.0	0.912816	0.037136	-520.385	-21.171
0.1	0.728473	-0.128758	-415.293	73.403
0.3	0.139701	-0.890105	-79.642	507.438

Table 4: The effects of M and n on -F" (0), -θ' (0) and -φ' (0) along their associated Cf_x, Nu and Sh number when α = N = 0.50, Le = 2.0, Pr = 6.20, Nt = Nb = 0.10 and λ = 0.20

M	n	-F" (0)	-θ' (0)	φ' (0)	Cf_x	Nu	Sh
0.1	0.5	1.050624	0.401282	0.443852	0.002573	-245.734	-271.803
0.5	1.0	1.224741	0.263455	0.419551	0.003464	-186.291	-296.667
1	1.5	1.340763	0.192773	0.399121	0.004240	-152.400	-315.533
1.5	0.5	1.754191	-0.004712	0.700332	0.004297	2.885	-428.864
3	1.0	2.000000	-0.156534	0.726977	0.005657	110.686	-514.050
10	1.5	2.972853	-0.409837	0.886594	0.009401	324.005	-700.914

Table 5: The effects of α and n on -F" (0), -θ' (0) and -φ' (0) along their associated Cf_x, Nu and Sh number when M = 1.0, N = 0.50, Le = 2.0, Pr = 6.20, Nt = Nb = 0.10 and λ = 0.20

α	n	-F" (0)	-θ' (0)	φ' (0)	Cf_x	Nu	Sh
0.2	-0.3	1.832473	-0.695121	1.686735	0.003066	290.790	-705.612
	0.3	1.534981	0.144619	0.661414	0.003500	-82.446	-377.064
	0.5	1.489362	0.203473	0.583602	0.003648	-124.601	-357.382
0.5	-0.3	2.181240	0.725677	0.605824	0.003650	-303.572	-253.434
	0.3	1.622922	0.329210	0.572688	0.003701	-187.679	-326.482
	0.5	1.541786	0.305178	0.540032	0.003777	-186.883	-330.701

RESULTS AND DISCUSSION

This study, concerned about the mathematical model of a nanofluid flow and heat transfer over a stretching sheet with nonlinear velocity along the flow field with both Brownian motion and thermal radiation being present. The influence of all the pertinent parameters involved in the velocity, temperature and nanoparticles volume fraction within the boundary layer has been presented in Fig. 2-11. Whereas, the effects of some related parameters in the temperature and volume fraction gradients at the surface along with the values of Nu and Sh at Re = 5×10^5 are duly exhibited in Table 2-5.

The accuracy between the present and previous studies has been juxtaposed in Table 1 where a very fascinate agreement between the two results have attained. The impact of thermophoresis parameter Nt on the temperature and nanoparticles concentration gradients with their associated values of Nusselt number and Sherwood number has been unveiled in Table 2. where the increase in the values of thermophoresis parameter results to the increase in the heat and mass transfer rates. Moreover, both Nu and Sh have effectively increased as the values of Nt rises from (0.1-0.6) simultaneously. An increase in the values of the heat source parameter λ, resulted to the decrease in the heat and mass transfer rates, Nusselt number and Sherwood number from the surface. But the Sherwood number has begins to ascend as the value of λ improves from (0.1-0.3) as contained in Table 3. The effects of magnetic field parameter M and shape parameter n on the velocity, temperature and nanoparticles volume fraction gradients at the surface along with proportionate values of Cf_x, Nu and Sh are presented in Table 4. It is clear that the increase in the values of both M and n leads to the increase in the surface shear stress while the dimensionless mass transfer rate decreases as M changes from (0.1-1) but as M and n move from (1.5-10) and (0.5-1.5) then it started ascending. Besides, the dimensionless heat transfer rate rapidly decreases with increase in both M and n. Where the skin friction, the Nusselt number and the Sherwood number have all increased.

Table 5 has shown how the velocity power index parameter (known as shape parameter) n influences the values of the surface shear stress, dimensionless heat and mass transfer rates with their respective skin friction, Nusselt number and Sherwood number. As the value of n increases both the surface shear stress and dimensionless mass transfer rate decreased while due to the thermal radiation along the surface, the dimensionless heat transfer rate happens to be increasing. Moreover, the

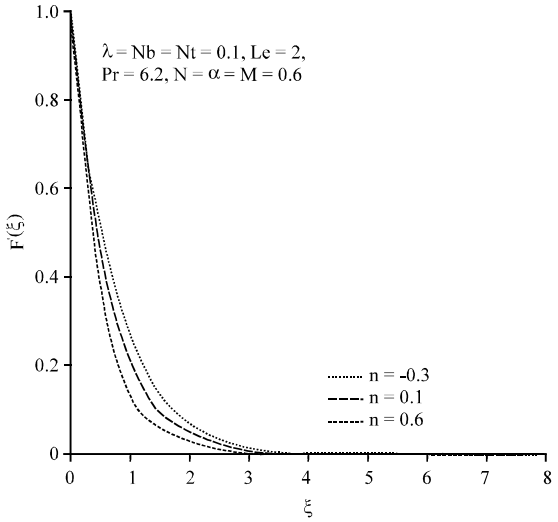

Fig. 2: Effect of shape parameter n on F'

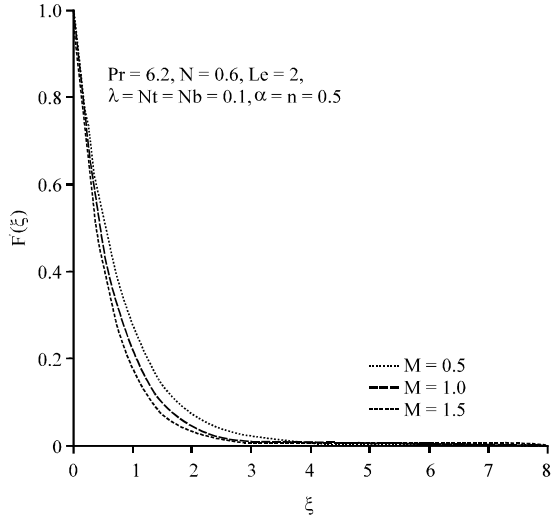

Fig. 3: Effect of magnetic parameter M on F'

skin friction has notably increases while the Nusselt number and Sherwood number were both decreasing due to the increase in the value of α as it moves from (0.2-0.5).

The shape parameter n has played a better role in controlling the surface shape, the category of shape as well as the nature of the boundary layer. Where it can be noticed that the external form of the surface absolutely depends on n values. As for n = 1, the study significantly diminishes to a flat surface with stable thickness. Whilst for n<1 this analysis remodelled into a surface with growing thickness and arched external shape. Albeit, for n>1 this analysis changes into surface with reduced thickness and recessed external shape. Moreover, for controlling the type of shape by this parameter such that

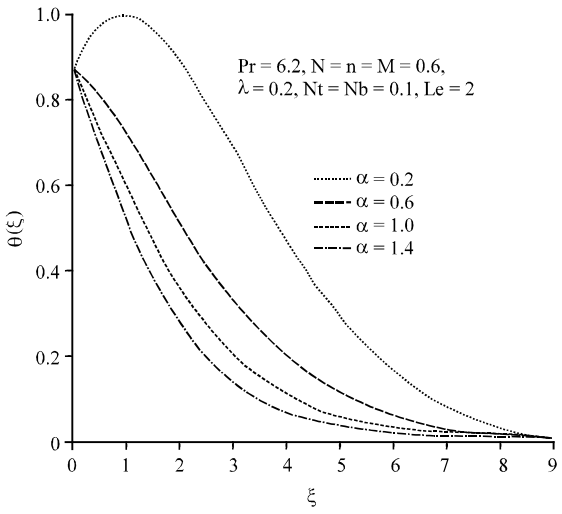

Fig. 4: Effect of thickness parameter α on θ

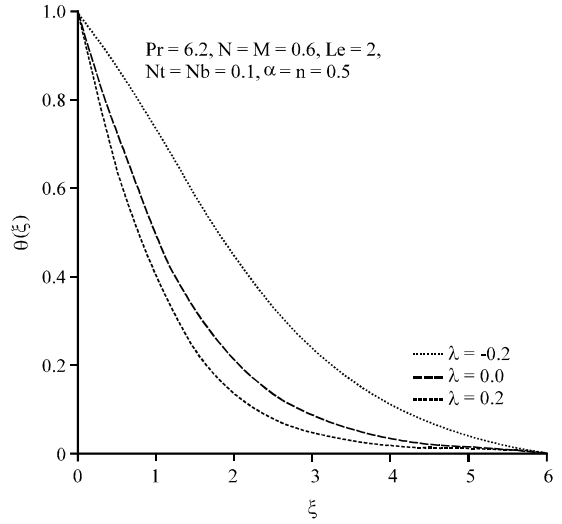

Fig. 5: Effect of heat source parameter λ on θ

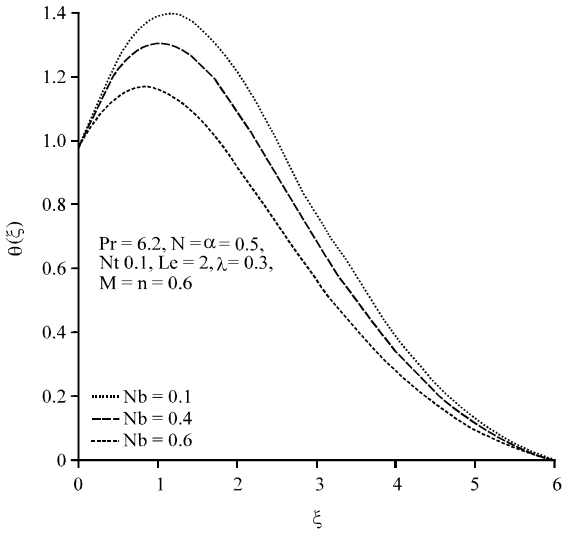

Fig. 6: Effect of Brownian parameter Nb on θ

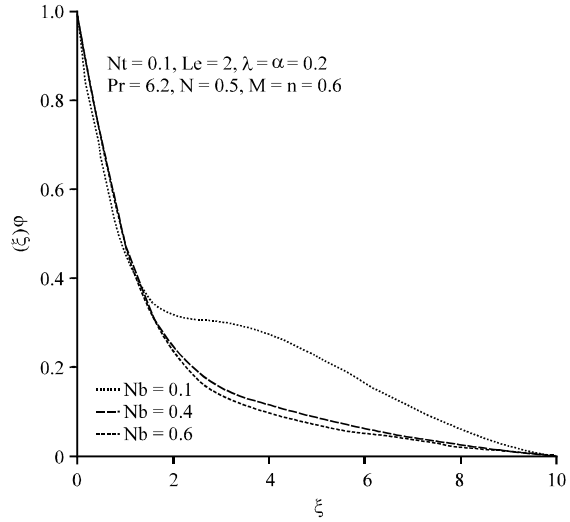

Fig. 7: Effect of Brownian parameter Nb on φ

for n = 0, the shape diminished to linear with uniform velocity but the shape slashed to retardation shape if n<1 and gives a hasten shape when n>1. Below are the graphical analyses of our results.

Figure 2 we have seen the impact of shape parameter on the velocity profiles and it is obvious that increasing the values of n leads to the increase of the boundary layer velocity. The effect of the magnetic parameter M on velocity profiles has shown in Fig. 3 where the velocity decreases with an increase of magnetic parameter M. Figure 4 is depicted the influence of thickness parameter α on temperature profiles as it is observed that the velocity decreases with an increase in the values of the thickness parameter. The effect of heat source parameter λ on temperature profiles as depicted in Fig. 5 shows that as the values of the heat source are increasing the boundary layer temperature is also increasing.

Figure 6 and 7 presented the influence of Nb on temperature and nanoparticles concentration profiles. Such that the increase in the values of Nb leads to the increase in the boundary layer temperature while the nanoparticles volume fraction decreases significantly. However, the temperature profiles have been affected by the presence of thermal radiation which drives to the increase in both the temperature and the thermal boundary layer thickness when N≤1 as depicted in Fig. 8 which exhibits the fascinate agreement between the two methods used. On the other hand, it has been noticed

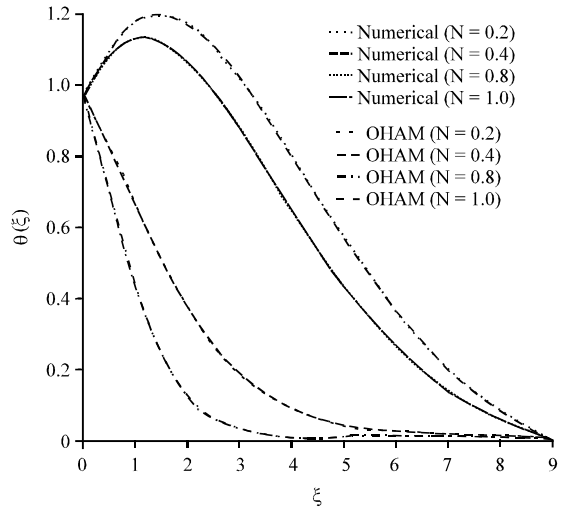

Fig. 8: Comparison between OHAM and numerical results at various values of radiation parameter N on θ when Pr = 6.2, n= M = 0.6, Nt = Nb = 0.1, λ = 0.2 and Le = 2

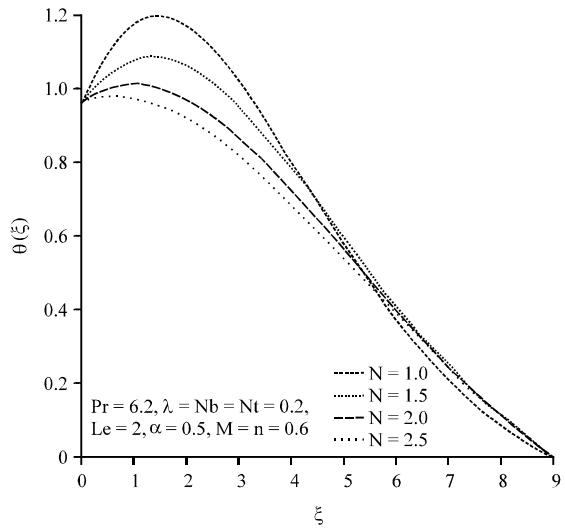

Fig. 9: Effect of radiation parameter N on θ

that the boundary layer temperature decreases when N>1 as presented in Fig. 9. The effect of the rmophoresis parameter Nt on temperature and nanoparticles concentration profiles is depicted in Fig. 10 and 11. Where it has been apparently observed that the temperature enhances vehemently when the values of Nt get stronger from (0.1-0.6). But the case was reversed on the nanoparticles concentration profile as the increase in the values of Nt results to increase in nanoparticles concentration.

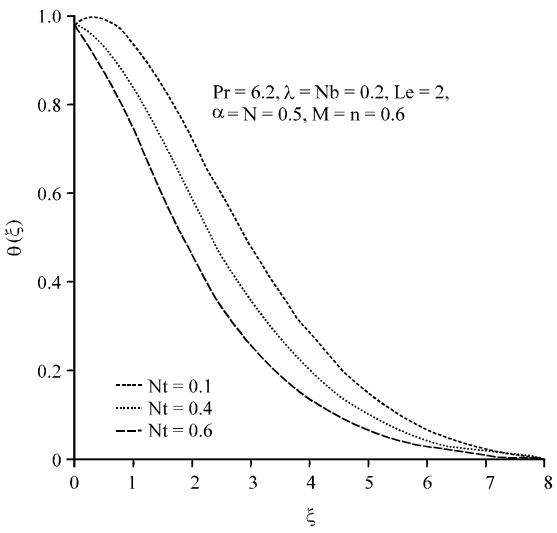

Fig. 10: Effect of thermophoresis parameter Nt on θ

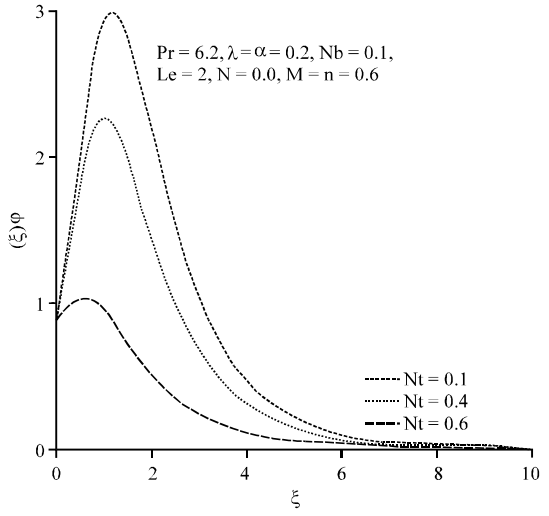

Fig. 11: Effect of thermophoresis parameter Nt on φ

CONCLUSION

In this study, we have examined the features of the heat and mass transfer over a dynamic stretching sheet with nonlinear velocity in a nanofluid with thermal radiation and Brownian motion influence. The impacts of all the related parameters on velocity, temperature and concentration profiles are shown graphically. Numerical results for the skin friction (surface shear stress), Nusselt number (surface heat transfer rate) and Sherwood number (surface mass transfer rate) are depicted in tabular form. The results can be summarized as follows.

The increase in the values of n results to the increase of the boundary layer velocity an increase in both Nb and Nt increases the temperature in the boundary layer province. While, the nanoparticle concentration increases with increase in Nt. Whereas, the nanoparticle volume fraction decreases significantly when the Nb increases the presence of radiation has a direct impact on the temperature profiles, where the temperature and the thermal boundary layer thickness increases when $N \leq 1$ and suddenly decreases when $N>1$.

ACKNOWLEDGEMENT

Researchers would like to express their profound gratitude to the Universiti Tun Hussein Onn Malaysia for the financial aid received from the Grant GIPS/FRGS/1434/U191 and RSGS/U112.

REFERENCES

Abdel-Wahed, M.S., E.M.A. Elbashbeshy and T.G. Emam, 2015. Flow and heat transfer over a moving surface with non-linear velocity and variable thickness in a nanofluids in the presence of Brownian motion. Appl. Math. Comput., 254: 49-62.

Akbar, N.S., S. Nadeem, R.U. Haq and Z.H. Khan, 2013. Radiation effects on MHD stagnation point flow of nano fluid towards a stretching surface with convective boundary condition. Chin. J. Aeronaut., 26: 1389-1397.

Ali, M.E., 1995. On thermal boundary layer on a power-law stretched surface with suction or injection. Int. J. Heat Fluid Flow, 16: 280-290.

Alsaedi, A., M. Awais and T. Hayat, 2012. Effects of heat generation-absorption on stagnation point flow of nanofluid over a surface with convective boundary conditions. Commun. Nonlinear Sci. Numer. Simul., 17: 4210-4223.

Ashraf, M. and M. Rashid, 2012. MHD boundary layer stagnation point flow and heat transfer of a micropolar fluid towards a heated shrinking sheet with radiation and heat generation. World Appl. Sci. J., 16: 1338-1351.

Chen, C.K. and M.I. Char, 1988. Heat transfer of a continuous, stretching surface with suction or blowing. J. Mathematical Anal. Appl., 135: 568-580.

Chiam, T.C., 1995. Hydromagnetic flow over a surface stretching with a power-law velocity. Int. J. Eng. Sci., 33: 429-435.

Choi, S.U.S., 1995. Enhancing Thermal Conductivity of Fluids with Nanoparticles. In: Developments and Applications of Non-Newtonian Flows, Siginer, D.A. and H.P. Wang (Eds.). American Society of Mechanical Engineers, New York, pp: 99-105.

Cortell, R., 2008. Effects of viscous dissipation and radiation on the thermal boundary layer over a nonlinearly stretching sheet. Phys. Lett. A, 372: 631-636.

Eid, M.R., 2016. Chemical reaction effect on MHD boundary-layer flow of two-phase nanofluid model over an exponentially stretching sheet with a heat generation. J. Mol. Liq., 220: 718-725.

El-Arabawy, H.A., 2003. Effect of suction/injection on the flow of a micropolar fluid past a continuously moving plate in the presence of radiation. Intl. J. Heat Mass Transfer, 46: 1471-1477.

Elbashbeshy, E.M. and D.A. Aldawody, 2010. Heat transfer over an unsteady stretching surface with variable heat flux in the presence of a heat source or sink. Comput. Math. Appl., 60: 2806-2811.

Elbashbesy, E.M.A. and M.A.A. Bazid, 2000a. The effect of temperature-dependent viscosity on heat transfer over a continuous moving surface. J. Phys. D: Applied Phys., 33: 2716-2721.

Elbashbeshy, E.M.A. and M.A.A. Bazid, 2000a. Heat transfer over a continuously moving plate embedded in non-Darcian porous medium. Intl. J. Heat Mass Transfer, 43: 3087-3092.

Elbashbeshy, E.M.A. and M.A.A. Bazid, 2003. Heat transfer over an unsteady stretching surface with internal heat generation. Appl. Math. Comput., 138: 239-245.

Elbashbeshy, E.M.A. and M.A.A. Bazid, 2004. Heat transfer in a porous medium over a stretching surface with internal heat generation and suction or injection. Appl. Math. Comput., 158: 799-807.

Elbashbesy, E.M.A. and M.A.A. Bazid, 2000a. The effect of temperature-dependent viscosity on heat transfer over a continuous moving surface. J. Phys. D: Applied Phys., 33: 2716-2721.

Fang, T., 2008. Flow and heat transfer characteristics of boundary layers over a stretching surface with a uniform-shear free stream. Int. J. Heat Mass Transf., 51: 2199-2213.

Fang, T., J. Zhang and Y. Zhong, 2012. Boundary layer flow over a stretching sheet with variable thickness. Appl. Math. Comput., 218: 7241-7252.

Hamad, M.A.A., 2011. Analytical solution of natural convection flow of a nanofluid over a linearly stretching sheet in the presence of magnetic field. Int. Commun. Heat Mass Transfer, 38: 487-492.

Hayat, T., I. Ullah, A. Alsaedi and M. Farooq, 2017. MHD flow of Powell-Eyring nanofluid over a non-linear stretching sheet with variable thickness. Results Phys., 7: 189-196.

Ishak, A., R. Nazar and I. Pop, 2009. Heat transfer over an unsteady stretching permeable surface with prescribed wall temperature. Nonlinear Anal., 10: 2909-2913.

Kandasamy, R., I. Muhaimin, A.B. Khamis and R.B. Roslan, 2013. Unsteady Hiemenz flow of Cu-nanofluid over a porous wedge in the presence of thermal stratification due to solar energy radiation: Lie group transformation. Intl. J. Therm. Sci., 65: 196-205.

Khan, U., S.T. Mohyud Din and B. Bin Mohsin, 2015. Convective heat transfer and thermo-diffusion effects on flow of nanofluid towards a permeable stretching sheet saturated by a porous medium. Aerosp. Sci. Technol., 50: 196-203.

Khan, W.A. and I. Pop, 2010. Boundary-layer flow of a nanofluid past a stretching sheet. Int. J. Heat Mass Transfer, 53: 2477-2483.

Kothandapani, M. and J. Prakash, 2015. Effects of thermal radiation parameter and magnetic field on the peristaltic motion of Williamson nanofluids in a tapered asymmetric channel. Int. J. Heat Mass Transfer, 81: 234-245.

Madaki, A.G., M. Abdulhameed, M. Ali and R. Roslan, 2016. Solution of the Falkner-Skan wedge flow by a revised optimal homotopy asymptotic method. Springer Plus, 5: 513-513.

Magyari, E. and B. Keller, 2000. Exact solutions for self-similar boundary-layer flows induced by permeable stretching surface. Eur. J. Mech. B/Fluids, 19: 109-122.

Marinca, V. and N. Herisanu, 2008. Application of optimal homotopy asymptotic method for solving nonlinear equations arising in heat transfer. Intl. Commun. Heat Mass Transfer, 35: 710-715.

Mustafa, M., A. Mushtaq, T. Hayat and A. Alsaedi, 2015. Radiation effects in three-dimensional flow over a bi-directional exponentially stretching sheet. J. Taiwan Inst. Chem. Eng., 47: 43-49.

Nadeem, S., A. Hussain and M. Khan, 2010. HAM solutions for boundary layer flow in the region of the stagnation point towards a stretching sheet. Commun. Nonlinear Sci. Numer. Simul, 15: 475-481.

Nazar, R., N. Amin, D. Filip and I. Pop, 2004. Unsteady boundary layer flow in the reagion of the stagnation point on a stretching sheet. Int. J. Eng. Sci., 42: 1241-1253.

Oztop, H.F. and E. Abu-Nada, 2008. Numerical study of natural convection in partially heated rectangular enclosures filled with nanofluids. Int. J. Heat Fluid Flow, 29: 1326-1336.

Pourmehran, O., M. Rahimi-Gorji and D.D. Ganji, 2016. Heat transfer and flow analysis of nanofluid flow induced by a stretching sheet in the presence of an external magnetic field. J. Taiwan Inst. Chem. Eng., 65: 162-171.

Prasad, K.V., D. Pal and P.S. Datti, 2009. MHD power-law fluid flow and heat transfer over a non-isothermal stretching sheet. Commun. Nonlinear Sci. Numer. Simul., 14: 2178-2189.

Prasad, K.V., K. Vajravelu and P.S. Datti, 2010. The effects of variable fluid properties on the hydro-magnetic flow and heat transfer over a non-linearly stretching sheet. Intl. J. Therm. Sci., 49: 603-610.

Rana, P. and R. Bhargava, 2012. Flow and heat transfer of a nanofluid over a nonlinearly stretching sheet: A numerical study. Commun. Nonlinear Sci. Numer. Simulat., 17: 212-226.

Rosseland, S., 1931. Astrophysik and Atom-Theorestische Grundlagen. Springer, Berlin, Germany,.

Sui, J., L. Zheng and X. Zhang, 2016. Boundary layer heat and mass transfer with Cattaneo-Christov double-diffusion in upper-convected Maxwell nanofluid past a stretching sheet with slip velocity. Intl. J. Therm. Sci., 104: 461-468.

Vajravelu, K., 2001. Viscous flow over a nonlinearly stretching sheet. Appl. Math. Comput., 124: 281-288.

Zhang, Y., M. Zhang and Y. Bai, 2016. Flow and heat transfer of an Oldroyd-B nanofluid thin film over an unsteady stretching sheet. J. Mol. Liq., 220: 665-670.